Development of mechanical guidance actuators for a supersonic projectile

K. C. Massey, J. McMichael, T. Warnock and F. Hay
Georgia Tech Research Institute,
Atlanta, USA

ABSTRACT

In this paper, the results of a series of experiments funded by DARPA to determine the feasibility of using small actuators to provide directional control for a supersonic projectile are presented. Controlling the flight of the projectile was accomplished by taking advantage of complex shock-boundary-layer interactions produced by mechanical devices. Experimental tests were conducted at GTRI to screen several control concepts and actuator locations. Further experiments were conducted on a scale projectile in a supersonic stream to investigate the rise time of the forces. Several different mechanical actuators were tested which served to provide guidance for future actuator designs. CFD results were also used to predict the results in flight as well as gain insights into the fluid mechanics involved. Flight tests of a Mach 4 round proved the viability of the guidance actuator.

NOMENCLATURE

AOA	angle-of-attack
M	Mach number
P	pressure
ΔX	lateral offset of pin from fin
ΔY	stream wise distance of pin from fin trailing edge

1.0 INTRODUCTION

There has been a recent interest in both missiles and guided projectiles that operate in the high supersonic to hypersonic range for various missions. The Office of Naval Research in the US has been pursuing HyFly[1] which is a proposed Mach 6 missile that would be used to strike targets of opportunity in a timely fashion before they could reposition. Marx *et al*[2]. discuss small guided projectiles that are under consideration for the future Objective force. They discuss how the increased lethality of guided projectiles will improve the survivability of the future soldier. Another area of interest revolves around cruise missile defense such as DARPA's low cost cruise missile defense (LCCMD) program and the Army's enhanced area air defense system (EAADS). One possible scheme for missile defense assumes that medium caliber guns with high rates of fire could fire multiple supersonic projectiles that could be guided into an incoming missile that may be undergoing evasive action. Warnash and Killen[3] describe several military programs where high speed guided munitions are in development or are under consideration. In all cases, it is found that the high closure rates between the projectile and the target may necessitate large turning forces.

It was the goal of this effort to provide an initial feasibility study into the use of strategically located actuators to provide the turning force needed to terminally steer a missile or

Paper No. 3210. Manuscript received 2 July 2007, revised 26 March 2008, accepted 28 March 2008.

https://doi.org/10.1017/S0001924000002128 Published online by Cambridge University Press

projectile. Initially only jet actuators were considered. These jets were not intended to be simple reaction jets, but were intended to modify the flow around the projectile in such a way as to greatly enhance the force on the body of the projectile. As the research progressed, the use of deployable pins was also evaluated to generate turning forces. Efforts were made to understand the physics behind these turning forces so that the lessons learned here could be applied to future missile and projectile geometries.

2.0 PRIOR WORK

Experimental studies that involve jets in supersonic cross flows have been pursued for nearly 60 years and thus there are too many works to cite here. Margason[4] provides an excellent review of many of the experimental studies. Spaid and Cassel[5] examine the particular case of *Aerodynamic Interference Induced by Reaction Controls* and correlate the pertinent experimental data over a wide range of Mach numbers and Reynolds numbers. As pointed out by Hemsch[6] and by Hsia[7], the basic fluid dynamic interactions of a solid body, or a jet, in a supersonic cross-flow are essentially the same, as a jet provides blockage to the flow. In both cases the influence of the jet, or solid object, is felt upstream due to a thickening of the boundary layer. This is shown in Fig. 1 where the upper sketch shows how the thickening of the boundary layer leads to an upstream separation shock and a downstream recirculation zone. In the lower portion of Fig. 1, the pressure field associated with this disturbance is shown. Upstream there is a rise in pressure associated with the shock, while downstream there is a low pressure region associated with the recirculation zone. The ratio of the rise in pressure was shown by Spaid and Cassel[5] to collapse as a function of Mach number as shown in Fig. 2 for Mach numbers from 1·5 to 13. In the same reference, Spaid and Cassel also showed that the geometric extent of the pressure disturbance could also be collapsed with appropriate Mach number scaling. While all of these experimental results were for a flat plate, it demonstrates that the pressure disturbances generated at one flight condition can be related to those of another flight condition through appropriate scaling.

Much of the initial work on jets in a cross flow was done in the 60s and 70s and was related to reaction control jets (RCJs) on missiles and ballistic vehicles. The nature of these studies was to examine the impact of RCJs on the overall flowfield around the body. One of the more interesting works in this field was by Champigny[8], where many different parameters of RCJs were experimentally explored. Variations such as the pressure ratio, gas temperature, injection port geometry, injection port orientation, injection port location, flight Mach number and other permutations were explored. Of particular relevance to the present study, he showed that the effect of the RCJ location relative to the missile fins strongly affected the missile pitching moment.

Recent work has focused both on the mixing phenomena associated with jets in regard to developing supersonic combustors and in manoeuvring projectiles. Much of the more recent work with regards to jets in a cross flow has been numerical in nature such as that of Schetz, *et al*[9]. and Fujimori, *et al*[10] The effects of different gas densities, such as injecting hydrogen into air have also been explored by Takahashi[11] and others. Several recent research efforts on manoeuvring projectiles such as the UK HOTLiP program[12] and Army Research Lab efforts have also been numerical in nature. Graham and Weinacht validated their numerical scheme to predict a control jet interaction[13] and then used their method to examine the case of a finned projectile with control jets[14]. They demonstrated that there were significant interactions that could increase the aerodynamic pitching moments relative to the jet thrust alone.

3.0 OBJECTIVE OF STUDY

In the fall of 2001, GTRI initiated a DARPA funded study to investigate the feasibility of using our flow control expertise to develop techniques capable of enabling a supersonic projectile to undergo rapid manoeuvres. Based on the authors' experience and the available literature, the program attempted to develop jet actuators that would not rely solely on the thrust of a jet based actuator but would obtain a high force multiplier through aerodynamically influencing the flow around the body. The interactions between a jet and supersonic flow were fairly well understood, yet the influence on the aerodynamic characteristics of a missile or projectile were not. Previous work had shown that aerodynamic interactions between RCJs and the body could influence the pitching moments and lift in either a positive or negative fashion, but this work was very limited in scope. In the public literature, it appeared that few efforts had been made to design for a favourable jet interaction that would amplify the force input. It thus became the objective of this study to design such a system where an actuator could rapidly influence the flowfield around the missile or projectile to generate the forces needed to rapidly turn the body.

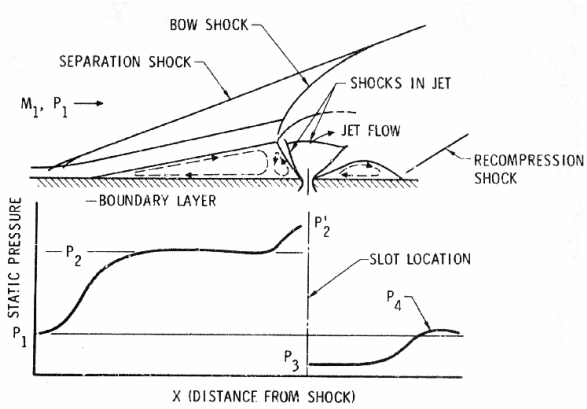


Figure 1. Flowfield and pressure distribution of supersonic jet in a supersonic cross-flow[5].

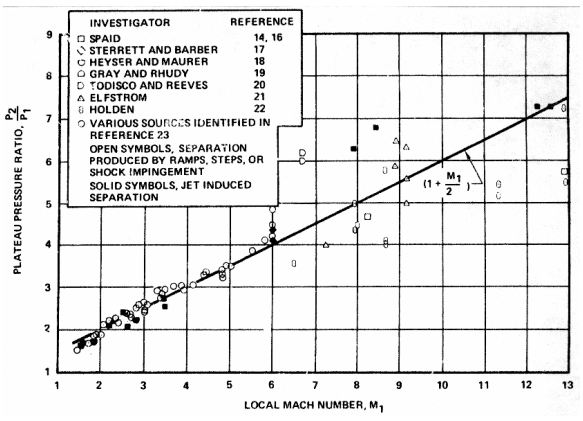


Figure 2. Correlation of plateau pressure rise with local Mach number[5].

https://doi.org/10.1017/S0001924000002128 Published online by Cambridge University Press

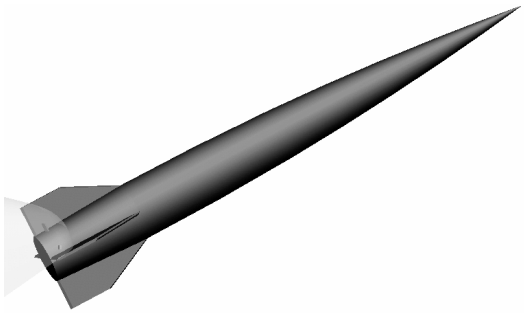


Figure 3. Pin fin concept.

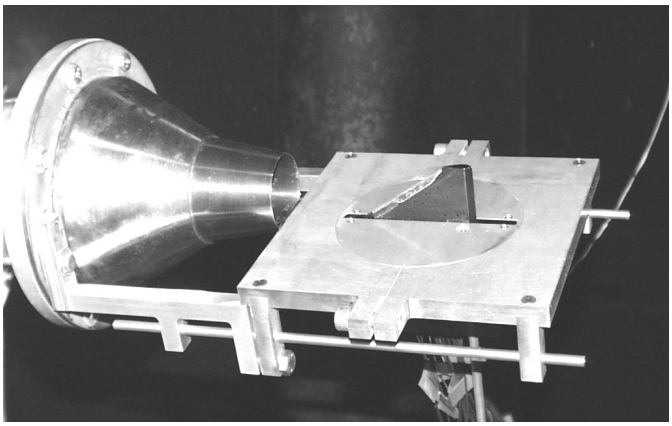


Figure 4. Installed hardware of fin interaction experiment.

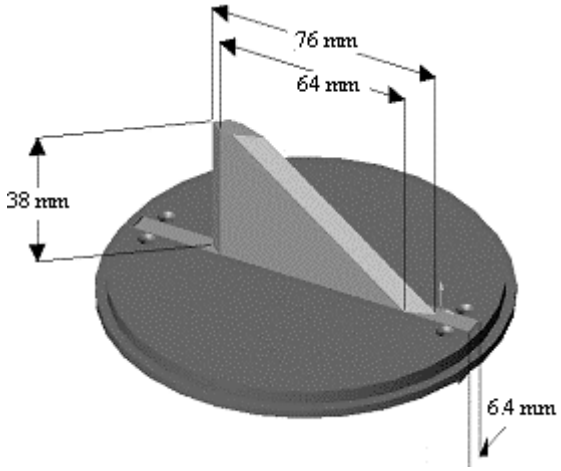


Figure 5. Dimensions of experimental fin.

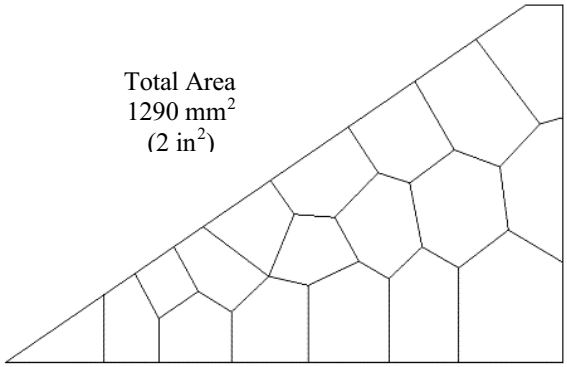


Figure 6. Pressure port layout and associated areas for experimental fin.

4.0 PIN FIN CONCEPT AND EXPERIMENTAL EVALUATION

4.1 Concept

Based on the lessons learned in previous efforts, a concept was developed to increase the force produced by properly locating the actuator. Building on the fact that the flow disturbance introduced by a jet or solid object inserted into the flow was three-dimensional in nature and extended away from the body of the projectile, it was hypothesised that if the actuator was moved close to a fin, not only would there be regions of high pressure generated on the body, but also on the fin as well. This is shown conceptually in Fig. 3 where a shock is created by an interaction between two pins and the flow. (Prior experiments had also shown that the use of pins was superior to that of jets particularly in the small form factor of a projectile.) In this conceptual image, the shock also has a large interaction with the fin as well as the body. Taking advantage of this 3D corner effect should enlarge the surface area of the projectile experiencing high pressure relative to positioning the actuator further away from the fins. One advantage to this concept is the fact that generating forces on the surfaces of the fins allows one to also control the roll rate of the projectile or missile. This enables the use of different control schemes that might not have otherwise been possible.

4.2 Test setup

To validate this concept a series of experimental tests and numerical studies were conducted. The first experimental tests used a simplified representative geometry that consisted of a fin on a flat plat immersed in a supersonic stream. The jet was a convergent divergent jet that could be operated at Mach 1·7 in a nearly shock free fashion. The fin was mounted onto a disk that could be rotated to change the angle-of-attack of the fin relative to the stream. A picture of this hardware mounted into GTRI's hot jet facility is shown in Fig. 4. The fin was designed to maximise its size while still allowing it to be immersed in the jet. As seen in Fig. 5, the fin was 38·1mm tall and 76·2mm long. The fin was instrumented with 18 pressure taps that were cut into the fin using a ram EDM (electrical discharge machining) process. The pressure port locations are shown in Fig. 6. The pressures measured from these pressure ports were used to estimate the force on the fin by assuming a constant pressure in the vicinity of the pressure ports. In Fig. 6, the areas used for these calculations are also shown. A series of seven holes where pins (¼ – 20 bolts)

https://doi.org/10.1017/S0001924000002128 Published online by Cambridge University Press

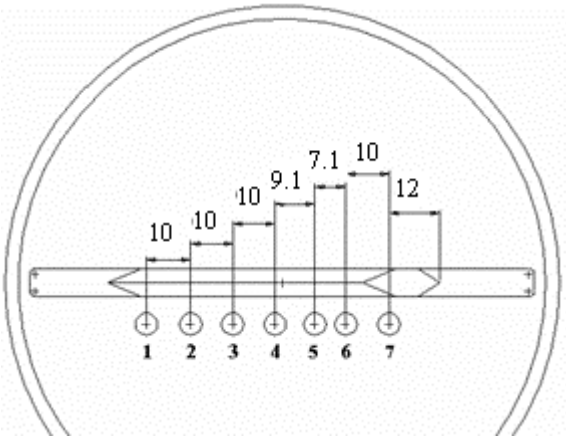


Figure 7. Dimensional spacing of pins and hole reference numbers.

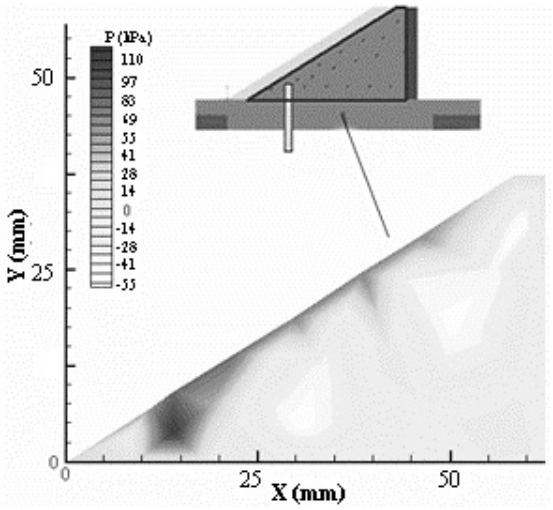


Figure 8. Generation of pressure contours on fin from experimental data.

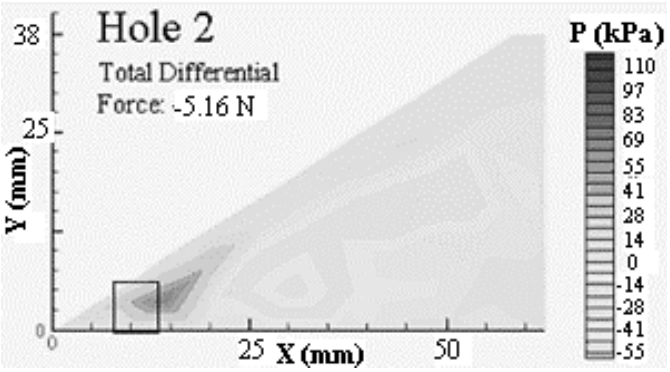


Figure 9. Fin pressure for 1 dia. height at Hole 2.

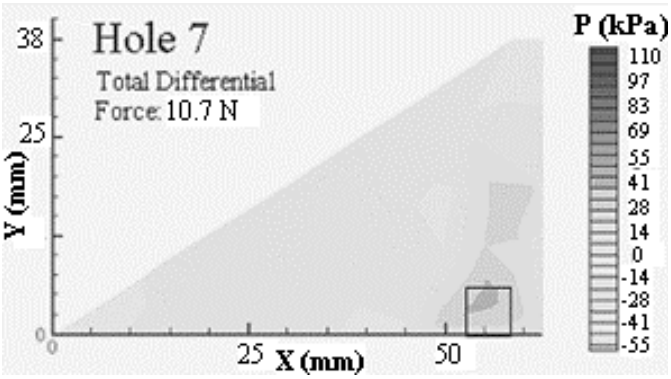


Figure 10. Fin pressure for 1 dia. height at Hole 4.

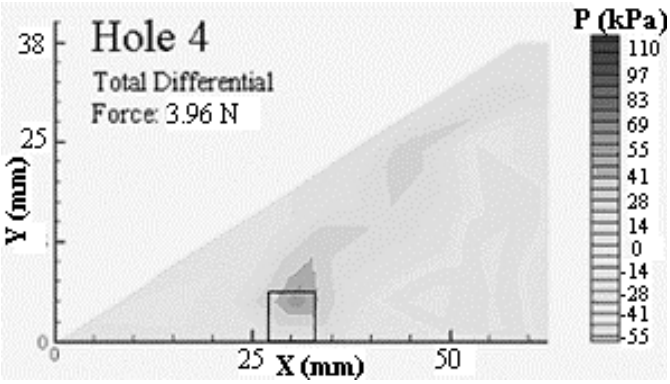


Figure. 11 Fin pressure for 1 dia. height at Hole 7.

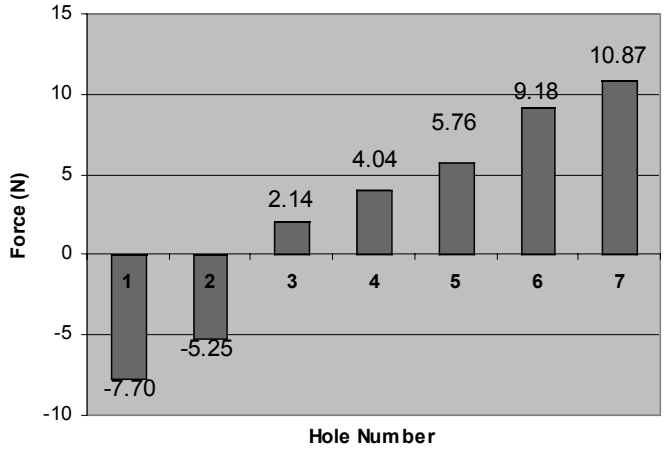


Figure 12. Differential forces for a 1 diameter height pin for various pin locations.

https://doi.org/10.1017/S0001924000002128 Published online by Cambridge University Press

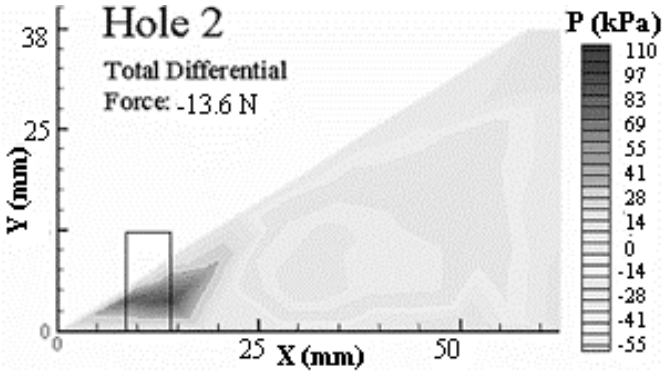


Figure 13. Fin pressure for 2 dia. height at Hole 2.

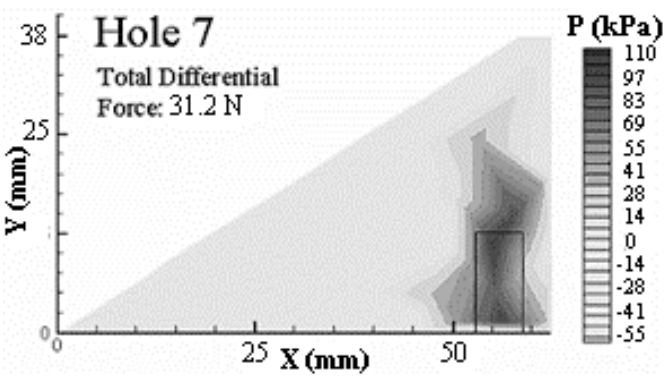


Figure 14. Fin pressure for 2 dia. height at Hole 7.

could be raised and lowered were tapped into the ground plane for a crude first approximation. The physical locations of these holes relative to the fin are shown in Fig. 7 where the reference number for each hole is also shown.

All of the pressures from the pressure ports were read simultaneously at a sampling rate of approximately 10Hz. These pressures were averaged over the course of three seconds using 30 samples. Each of the averaged pressure values was associated with a given area and thus the forces on these areas, shown in Fig. 6, could be calculated. Summing up these forces led to an estimation of the force on the fin. Note that only the surfaces parallel with the stream were used in these calculations as it was not feasible to measure the pressures on the tapered parts of the fin. Contour plots of the pressures on the instrumented surface of the fin were also generated as shown in Fig. 8.

The ¼ – 20 bolts allowed for rapid testing to determine the optimal streamwise location of the actuators as well as the penetration depth of the jet or pin that would be required. A series of tests were conducted where the pins were raised to three different heights at each of the seven hole locations. Pressure data was recorded for each of these runs. To insure that there was no effect on the other side of the fin, these tests were repeated with a mirror image set of holes on the other side of the fin. Measurements were made for three different pin insertion depths, 1 diameter, 2 diameters and 2·4 diameters, at all of the hole locations. Only a limited set of the data is shown here.

5.0 FLAT PLATE FIN RESULTS PART I

At the minimum insertion depth of one diameter, large changes were induced in the flow field which in turn drastically changed the pressures on the fin. As anticipated these pressure fields were characterised by a pressure increase in the vicinity of the pin and a downstream region of low pressure. These effects are shown quite clearly in Fig. 9 where the pressure levels on the fin when a pin was inserted at Hole 2 are shown. For this case, the pressure change due to the presence of the pin resulted in a net drop in pressure over the entire fin. While there was a pressure increase near the pin, the low pressure region downstream covers a larger area resulting in a net suction force of about 5N. One can also clearly see that the pressure changes are three dimensional in nature as virtually the entire fin is affected.

At pin positions further downstream, the pressure changes on the fin have essentially the same character with the pressure changes shifted downstream. With the pin at Hole 4, see Fig. 10, it is clearly seen that the low pressure region occurs further downstream than when the pin was at Hole 2. The pressure forces on the pin are roughly of the same magnitude for both Hole 2 and Hole 4, but the sum force is positive for Hole 4 while it is negative for Hole 2. This is due to the fact that the fin sees less of the low pressure region behind the pin. Figure 11 shows that this is even more evident when the pin is at Hole 7 where the low pressure region is not even felt by the fin. As would be expected, the pressure force is even higher for this case and was found to be 10·6N. A summary of the forces induced by a pin inserted to a height of 1 diameter is shown in Fig. 12. It is clear that the force is maximised as one moves the pin downstream thus eliminating the effects of the downstream separation.

When the height of the pin was increased to two diameters pressure changes on the fin were dramatically increased. These changes suggest that the shock structure was much stronger and produced both larger changes in pressure on the fin and increased the area affected by the shock interactions. In Fig. 13 data is shown for a 2 diameter height pin at Hole 2. Here it is seen that for the high pressure region the peak differential pressure is higher and that the low pressure region has lower pressures than for the corresponding 1 diameter height pin in Fig. 9. As a result, the total force on the fin is increased by roughly a factor of 3 to 13·3N. In Fig. 14, which shows the data for the 2 diameter height pin at Hole 7, it is seen that the extent of the pressure change is larger than for the 1 diameter height. For the 2 diameter height case, the pressure disturbance nearly extends to the top of the fin and it is thus likely that greatly increasing the pin height would provide diminishing returns in terms of increasing the force on the fin.

Further measurements were made using a slotted jet instead of the crude pins, with similar force contours. This data is not presented here as the contours are very similar. Essentially the same pressure forces could be generated with a jet that introduced the same level of flow disturbance as the pins. This, however, requires high pressures and exceedingly high mass flows as the Mach number of the free stream increases. For this reason, it was felt that the use of jets as opposed to mechanical pins did not make sense for a relatively small projectile.

As the force generation was intended to be used for manoeuvring a finned projectile, the fins would be at some angle-of-attack at some point during the manoeuvre. Experiments were thus conducted with the fins at various angles of attack relative to the flow. It was found that the forces on the fin were diminished with increasing angle-of-attack but only slightly. Using the 2 diameter height pin at Hole 7 as a baseline, pressure data was acquired for two other angles of attack. At 3° angle-of-attack, the total force was reduced from 31·2N to

https://doi.org/10.1017/S0001924000002128 Published online by Cambridge University Press

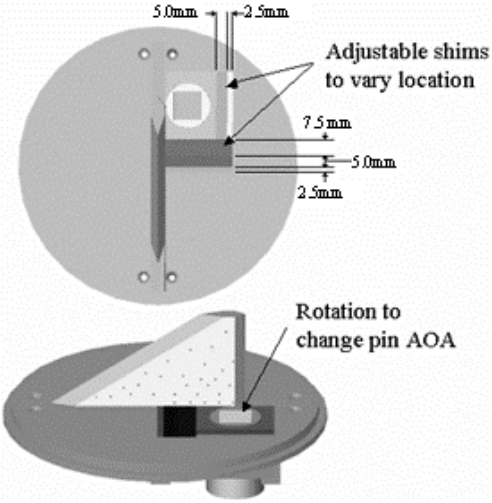


Figure 15. Second generation fin flat plate experimental setup.

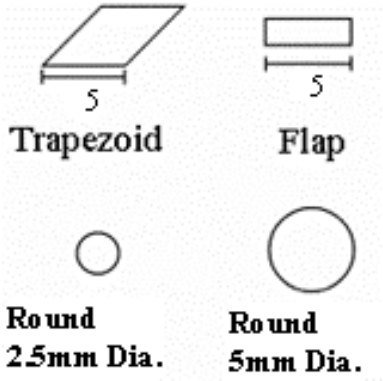


Figure 16. New pin shapes.

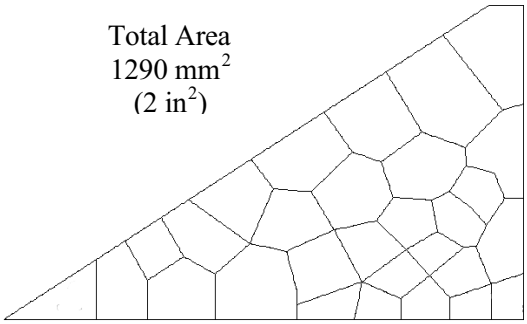


Figure 17. Second generation pressure port layout.

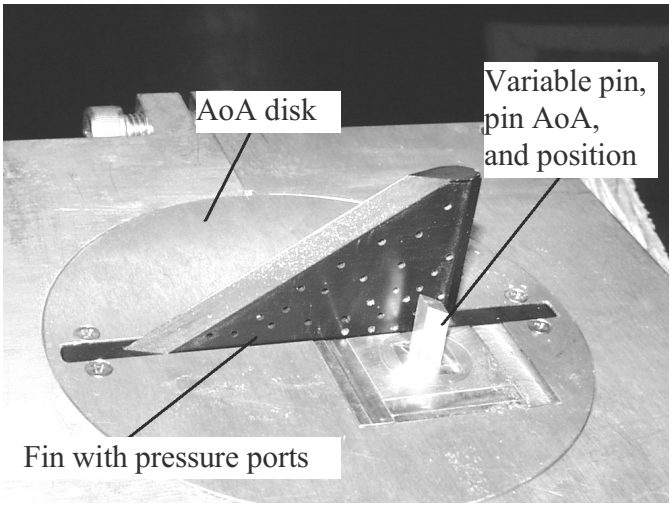


Figure 18 Experimental setup for pin shape and optimisation of pin location testing.

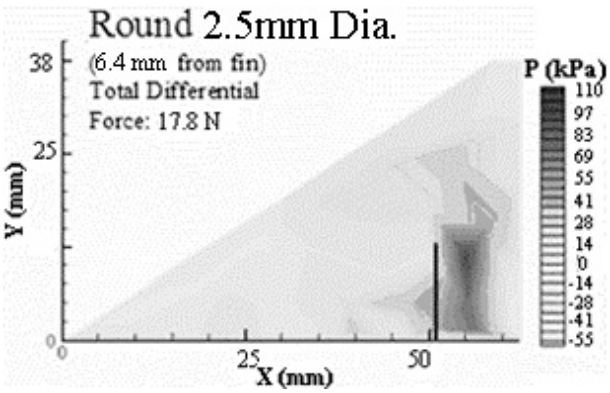


Figure 19. Fin pressure induced by 2.5mm dia., 5mm height round pin at 6·4mm from TE.

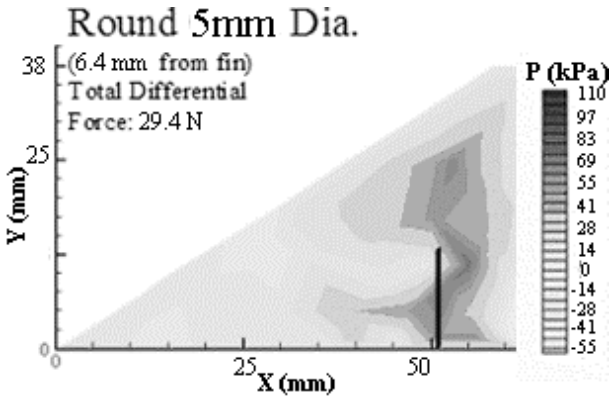


Figure 20. Fin pressure induced by 5mm dia., , 5mm height round pin at 6·4mm from TE.

https://doi.org/10.1017/S0001924000002128 Published online by Cambridge University Press

29·6N. It appeared that the localised region of very high pressure near the pin may be smeared out a little more, but that the larger region of high pressure did not extend as far forward at angle-of-attack. These observations are more evident at 5° angle-of-attack as the force level saw a further reduction to 28·4N, nevertheless the force levels at angle-of-attack still remained substantial.

6.0 FLAT PLATE FIN RESULTS PART II

After analysing the results from the initial Flat Plate Fin tests, it was decided to pursue the use of pins as actuators over jets. Several design changes were made and implemented in an effort to both improve the fidelity of the measured results and to further optimise the pin location.

Much of the same hardware was used as in the previous tests, but modifications were made to the flat plate that allowed for the pin to be moved both in the streamwise direction and normal to the fin direction. Since a rough optimal streamwise location was found in the previous tests, it was possible to fine-tune the adjustability in this direction. This setup, which is shown in Fig. 15, also allowed for the pin to be rotated. While this setup did not allow for infinite variability, it did allow us to further hone in on the optimal pin location and angle.

It was also felt that other pin geometries besides round pins could produce more force on the fin. In addition, these non round shapes might also produce a complementary force in the desired direction. Four different pins were tested in these experiments. Their cross-sectional shapes are shown in Fig. 16. The trapezoid shape was conceived in the hope of generating a complementary force on the pin. The flat plate, or flap pin, was tested to mimic the deflection of a flap near the trailing edge of the fin. The two round geometries were tested to provide some continuity to the previous tests and to verify if any benefits were actually achieved with the non-round pins.

Prior to making the experiments described in Part I, it was not known where on the fin would be the regions of high induced pressure. From these earlier experiments, it was known that the fidelity of the measurements could be improved if additional pressure ports were added in the vicinity of the pin. An additional ten pressure taps were added to the fin in this region for the next set of experiments. In Fig. 17, the new layout of the pressure ports can be seen. Comparing this layout with that of Fig. 6, the areas where pressure is assumed to be constant have been greatly reduced in the area where the largest pressure changes are expected. This change clearly results in an increased fidelity in the force calculations.

A picture of the trapezoid pin installed next to the modified fin and flat plate is shown in Fig. 18. Here it is possible to distinguish the new pressure taps added to the fin as the lighter coloured holes. (They are lighter in colour since the fin was not anodised after drilling the new holes.) The spacing plates and rotation mechanism for the pin can also be seen. The height of the pin relative to the fin is also shown. For all of these experiments, the pin height was set to 12·7 mm which was nominally 2·5 times the longest dimension of the pin.

Two of the pressure contours from the round pin results are shown in Fig. 19 and Fig. 20 for the 2·54 and 5·08mm diameter round pins, respectively. Qualitatively, they both resemble the results for the ¼ – 20 pin at a similar location shown in Fig. 14 and the force levels are similar for the 5mm diameter pin. It is interesting to note that the peak pressure amplitudes are greater for the smaller diameter pin as shown in Fig. 19, even though the overall force is 50% higher for the larger pin. This typifies the result that it is more important to influence a larger area of the fin as shown in Fig. 20.

Detailed studies into the optimal location and angle of the non-round pins were performed. The effect of angle-of-attack of the pin on the fin side force for both the flat and trapezoidal pins was measured over a range of angles. For these measurements, 0° angle-

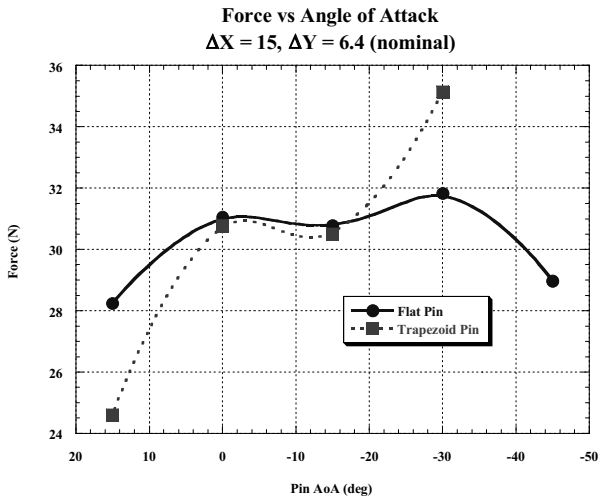


Figure 21. Effect of pin angle-of-attack on the pressure force generated on the fin.

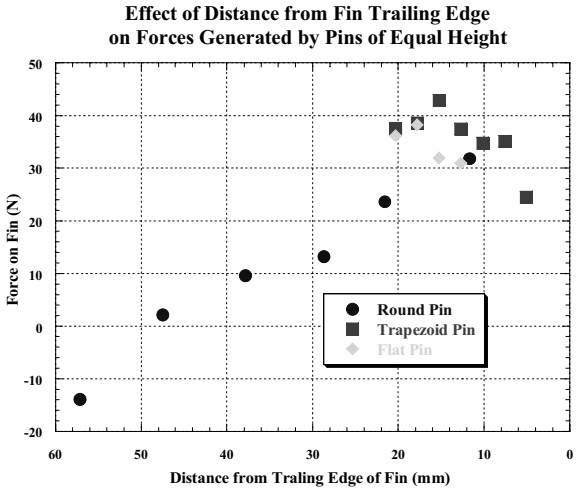


Figure 22. Effect of distance from trailing edge on force produced by pins.

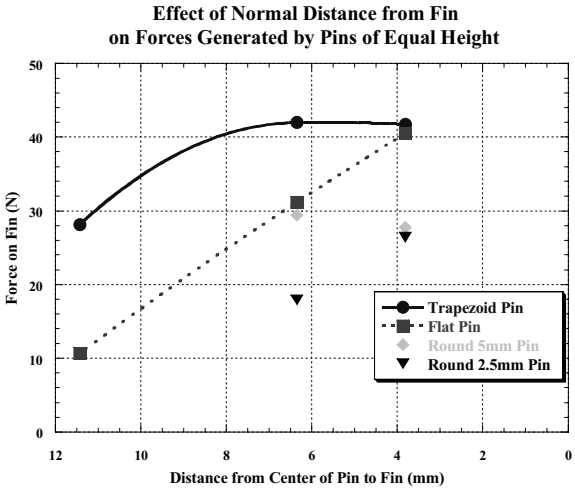


Figure 23. Effect of distance from fin on force generated by various pins.

https://doi.org/10.1017/S0001924000002128 Published online by Cambridge University Press

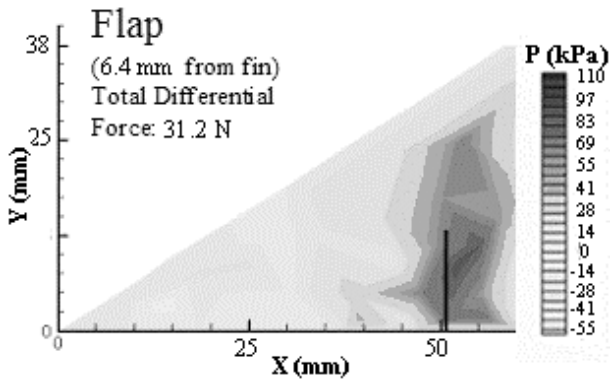


Figure 24. Fin differential pressure induced by 12·7mm height flat pin at 15mm from TE.

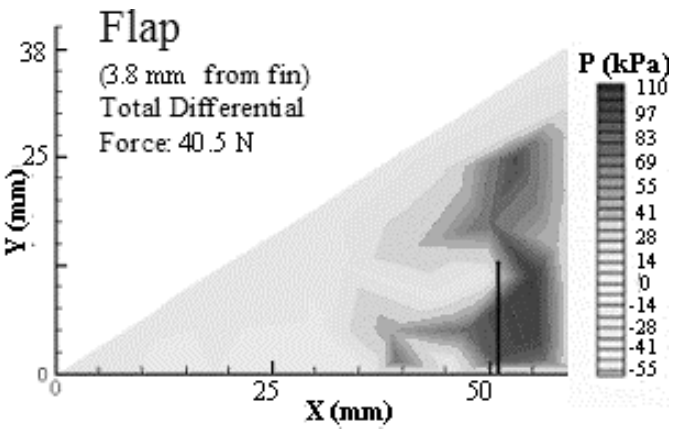


Figure 25. Fin differential pressure induced by 12·7mm height flat pin at 15mm from TE.

of-attack represented the case where the pin was oriented as shown in Fig. 16 and the flow was moving from the top to the bottom of the page. For positive angle-of-attack, the pin was rotated counter-clockwise. Figure 21 shows the effect of pin orientation on the pressure force exerted on the fin. The pin orientation does not have a very strong effect for the flat pin, while for the trapezoidal pin the force can vary by a factor of two depending on the orientation of the pin. Effectively the rotation of the pin resulted in a change in the pin frontal area presented to the flow. It is hypothesised that it is this frontal area which drives the flow disturbance which in turn drives the amount of force produced on the fin. For the trapezoid pin, an angle-of-attack of –30° was near the optimum orientation for force generation and thus this orientation was used for the remaining tests to optimise the pin location.

The previous efforts with the ¼ – 20 pins clearly demonstrated that the force level was increased as the pin was moved closer to the trailing edge of the fin. This increase in the force was found to be due to the fact that the low pressure region found downstream of the pin would occur off the body. Since similar results were expected for the non-round pins, the search range for the optimal pin location was narrowed. In Fig. 22, the force levels for the round pins (prior results), trapezoidal, and flat pins are shown as a function of distance from the fin trailing edge for a fixed pin height and separation distance from the fin. While the optimal location appears to vary slightly for the flat pin and the trapezoidal pin, in both cases it is near 16·5mm from the trailing edge. It is possible that this is also the optimal location for the round pin as well, though the data is too coarse to be positive.

The separation distance for the flat pin from the fin was found to strongly affect the force generated. As seen in Fig. 23, the force levels varied by a factor of four for the flat pin. For the trapezoidal pin, the force induced on the fin did not change noticeably as the pin was moved from 3·8mm from the fin to 6·4mm, however it rolled off rapidly for further separation. For the flat pin, there was a noticeable change in both the total forces and the pressure contours as the pin was moved perpendicularly away from the fin. In Fig. 24, the flat pin is 6·4mm from the fin while in Fig. 25, the pin has been moved closer to 3·8mm.

The second set of experiments testing a pin in proximity to a fin on a flat plate demonstrated that the force level produced by pins could be augmented by appropriate placement and orientation of a non-round pin. The use of non-round pins resulted in force levels that were 50% higher than for round pins. It was also shown that the streamwise location of a pin for maximum force generation was independent of the geometries tested. The results demonstrated that the force levels had a strong dependence upon the separation between the pin and the fin. There was some evidence that the force levels were reduced as portions of the pin entered the boundary-layer of the fin. The orientation of the pins was also shown by the experiments to introduce changes in the force level on the fin. A third set of experiments involving a flat plate and fin were conducted using a force balance and a further refined set of pins, as described by Hay and Massey[15]. The experimental results were very useful in optimising the location of the pins, however, they were lacking in predicting the total forces and moments that would be developed on a projectile. For that reason, CFD studies were conducted.

7.0 CFD OF PINS

CFD simulations were completed using CFD++[16] (Metacomp Technologies, 2000). CFD++ solves the Reynolds-averaged Navier-Stokes equations within a finite volume framework. The pointwise k-ε turbulence model[17] was used for the computation of the turbulent flow. Spatial discretisation is accomplished using the cell face normal at the cell face centroid, which is obtained by reconstructing the cell centroid values. The point-implicit integration scheme was used to solve the steady-state simulation.

Numerical simulations of the flow over a projectile with pins in both a roll control configuration, Fig. 26, and in a directional control configuration, Fig. 27, were conducted. For a single Mach number, both flat and trapezoidal pins were studied for a projectile at several small angles of attack. The orientation and the location of the pins were based on the experimental results described above. For this orientation of the pins, the trapezoidal pin has roughly 1·7 times the frontal area of the flat pin and thus generates more force. The surface pressures generated on the fin, pin, and body for the flat pin are shown in Fig. 28. Here the high pressures generated by an upstream shock similar in nature to that conceptualised in Fig. 3 are apparent. The region of increased pressure extends upstream to nearly ¾ of the fin height. Near the trailing edge of the body/fin juncture, a small region of low pressure exists due to separation behind the pin. It was desired to have this region completely off the body, and while this is mostly achieved, it might be possible to further optimise the location. For the same flow conditions, the pressure distribution for the trapezoidal pin configuration is shown in Fig. 29. For the most part, the pressure contours are quite similar between the two different geometries. However, it is possible to see that the region of increased pressure both extends further and is stronger for the trapezoid pin. The high pressure region extends all the way to the

https://doi.org/10.1017/S0001924000002128 Published online by Cambridge University Press

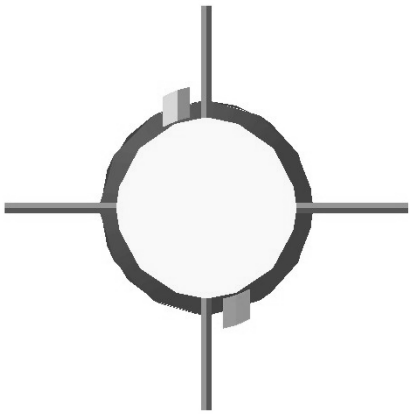


Figure 26. Pins used for roll control.

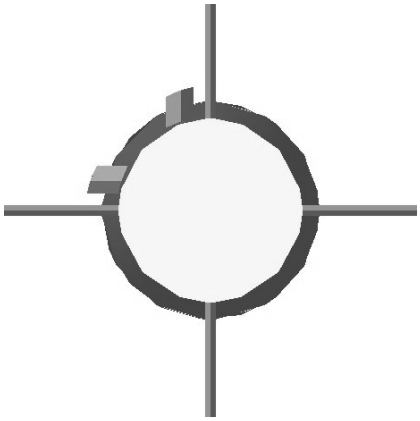


Figure 27. Pins used for directional control.

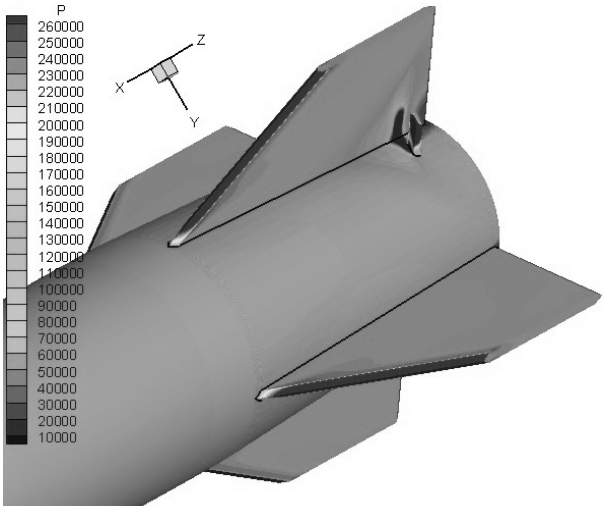


Figure 28. Surface pressures for flat pin with projectile at 0° angle-of-attack, roll control configuration.

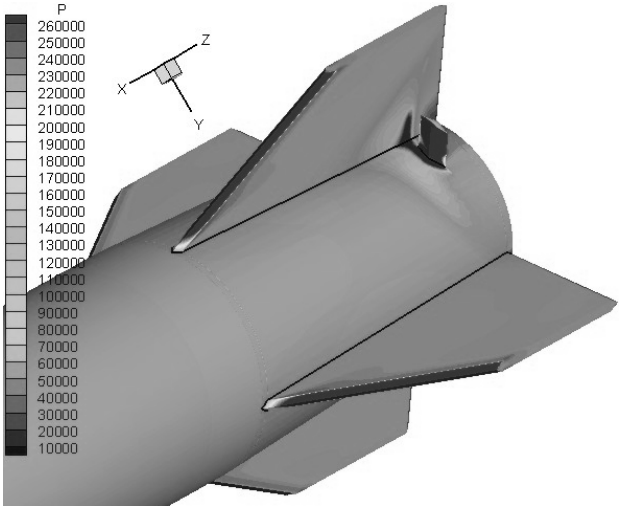


Figure 29. Surface pressures for trapezoid pin with projectile at 0° angle-of-attack, roll control configuration.

opposite fin for the trapezoid pin. On the other hand, the region of low pressure behind the pins is also more pronounced for the trapezoidal pin. In both cases there are extremely high pressures on both of the pins which will obviously result in increased drag. These high pressures are complemented by very low pressures on the leeward side of the pins. For a properly designed and oriented pin, it may be possible to take advantage of this situation to generate forces in a chosen direction.

By comparing the computationally derived pressure contours shown in Figs 28 and 29 with those described above using the experimental apparatus, it is found that the experimental and computational results are quite similar. The pitching moment developed by a pair of pins on a projectile based on the pin-flat plate experiments was estimated and the results were within 13% of the moment predicted by CFD. This is quite good especially when one considers that the geometries were different, the force on the body had to be estimated since it was not measured and that the drag of the pins as well as the force on the pins was not included in the estimation. We were therefore able to conclude that the experimental setup was a good screening tool and that the CFD was providing realistic results.

The rolling moments predicted by the CFD were quite large as the pins were sized more for directional control than roll control. With rolling moments of approximately 0·25N-m, the calculated angular roll rate accelerations are on the order of 4,000rad/s^2 assuming no aerodynamic forces and an axial moment of inertia of 580g-cm^2. Clearly these pins would enable rapid roll control and this was demonstrated on a gun range at the US Army Research Laboratory (ARL)[18].

Using the results from the CFD, it was possible to conclude that the use of pins could conceptually produce enough force and moment to implement a bank to turn type control scheme. 6DOF simulations based on the results described in this paper implementing such a concept are described by Massey, *et al*[19]. Several hurdles still remained. With all of the conclusions to date based on steady state experiments and CFD, it was not possible to accurately determine pitch and roll rates or how quickly the force would develop once the pins were deployed. Designing and packaging a system that would deploy the pins while fitting into a projectile remained a further challenge.

8.0 SCALE MODEL TESTS

Another series of experiments were conducted at GTRI involving the measurement of forces and moments on a scale model in a supersonic stream. There were three main goals of these tests: to determine the effect of pin height on force and moment, to

https://doi.org/10.1017/S0001924000002128 Published online by Cambridge University Press



Figure 30. Test article size reference.

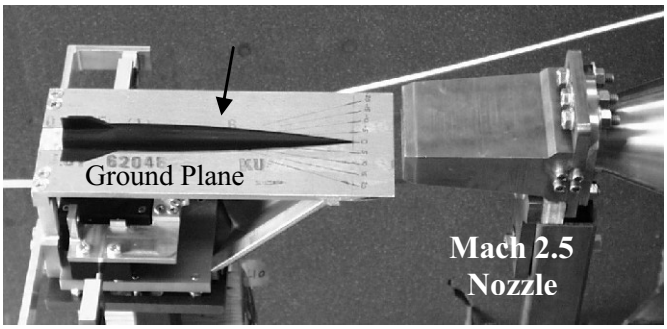


Figure 31. Top view of half model setup.

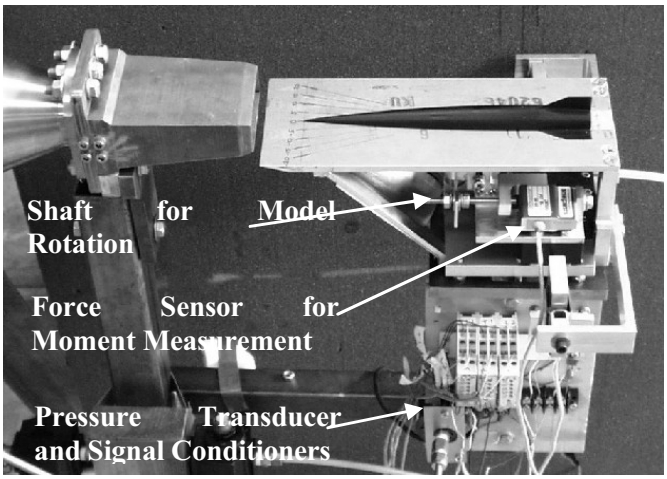


Figure 32. Instrumentation view of half model.

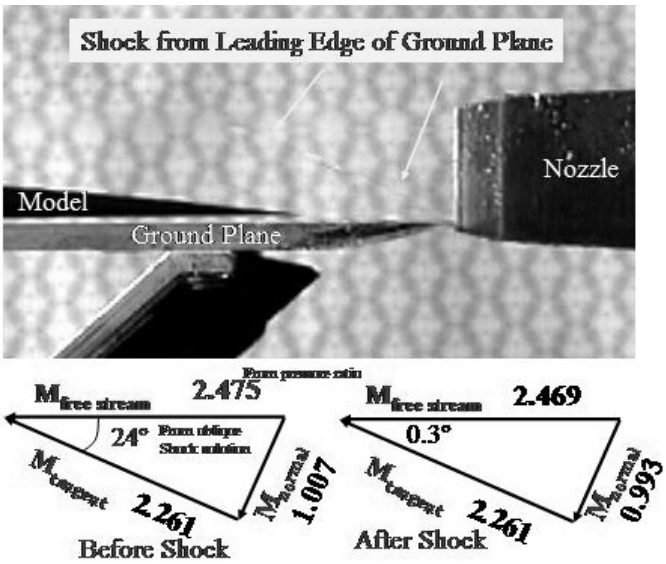


Figure 33. Shock introduced by ground plane.

estimate system response time, and to develop new ideas for how to package the system for final use. Steady force and moment measurements were made for a range of pin heights and orientations to determine their effect on force and moment. Time dependent force and moment data was acquired to gain estimates of the rise time of the forces and moments after deployment of a pin. Finally, practical experience was gained in designing and packaging a system to deploy pins.

8.1 Scale model hardware and setup

To measure the forces and moment introduced by a pin on the projectile under investigation, an experiment was designed where the full projectile was modeled as a full-scale half projectile on a ground plane. The projectile was split along a longitudinal line of symmetry that split two fins. This split line was chosen due to the constraints imposed by the one translational degree of freedom of the force balance.

The test article was cut out of a solid piece of aluminium using a six-axis CNC mill. The test article was later black anodised to protect the metal. Three views along with a scale are shown in Fig. 30. In the lower view, the underside of the test article is shown where several holes and cutouts are visible. The cutout near the nose was later filled with a machined block of tungsten to move the model cg forward. The threaded round hole in the center of the model was used to attach the model to the force balance. The model was trimmed such that the cg of the model was at this location. The aft slot was used to mount the actuator hardware and any additional weights needed to trim the model.

A Mach 2·5 convergent/divergent nozzle was designed and fabricated to create the supersonic stream over the projectile. The exit area of this nozzle was 76·2mm by 25·4mm (3in by 1in). The nozzle was supplied compressed and dried air at 2·07MPa (300psi) that was regulated by a 0·1m (4in) valve. A top view of the nozzle, ground plane and projectile is shown in Fig. 31. A view from the other side of the test assembly, Fig. 32, shows additional details such as the

https://doi.org/10.1017/S0001924000002128 Published online by Cambridge University Press

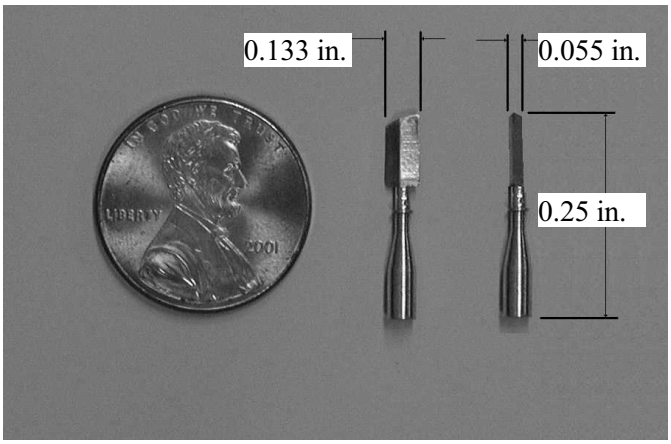


Figure 34. Trapezoid actuator size references.

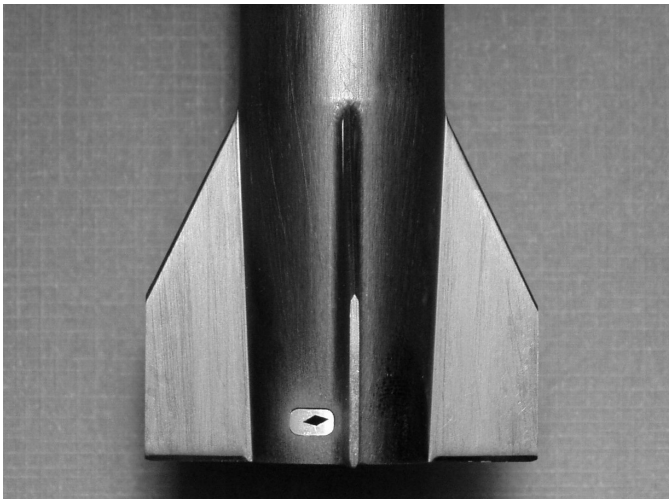


Figure 35. Pin AoA sleeve installed in model.

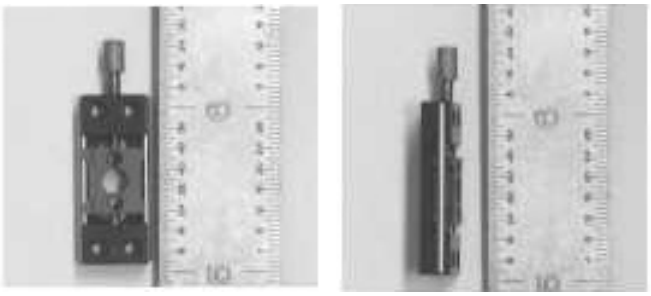


Figure 36. Manual actuator (MM1 micropostioner).

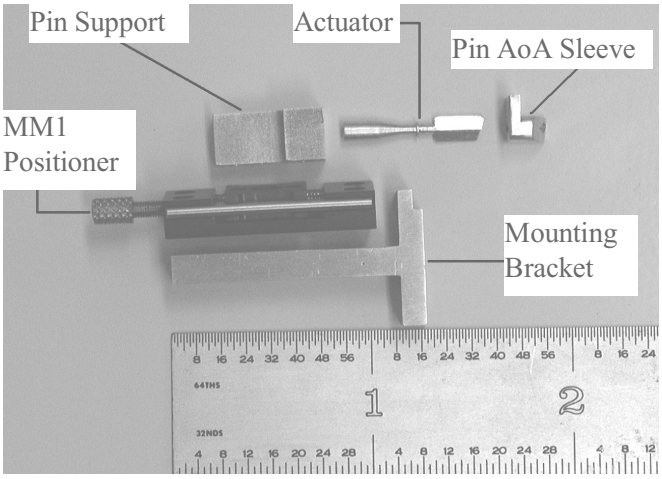


Figure 37. Exploded view of actuator parts.



Figure 38. Actuator retracted.

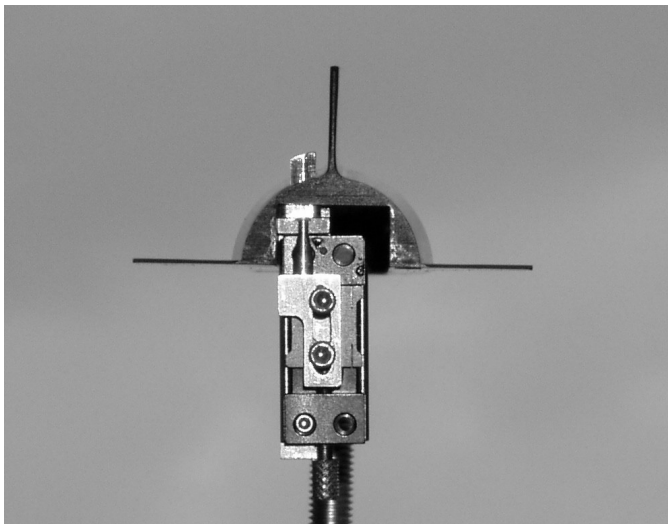


Figure 39. Actuator fully extended.

https://doi.org/10.1017/S0001924000002128 Published online by Cambridge University Press

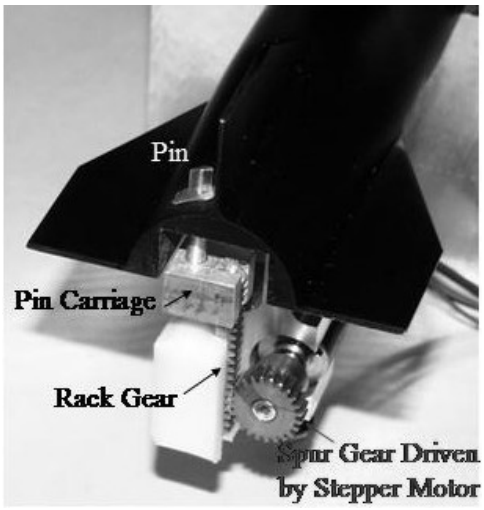


Figure 40. Rack and pinion actuator.

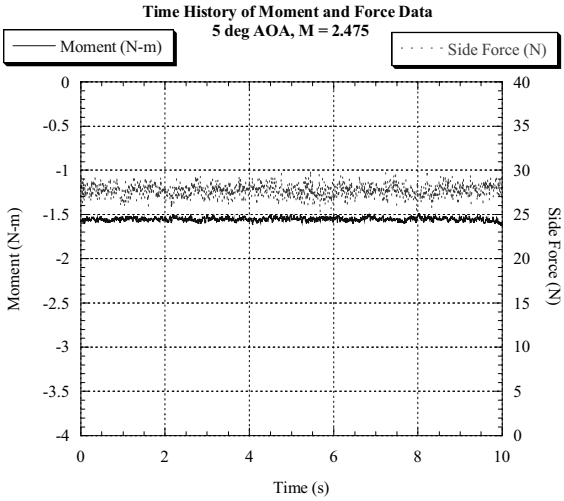


Figure 41. Time history of forces.

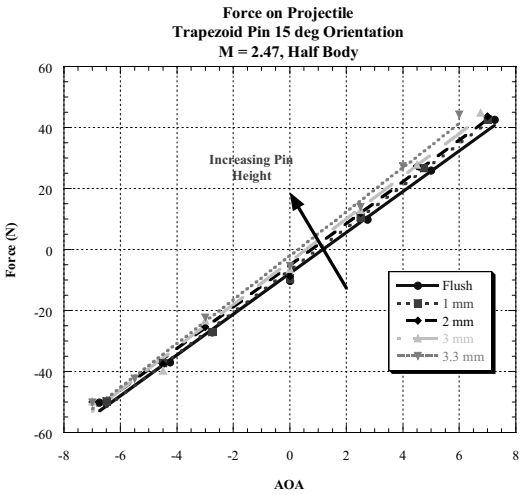


Figure 42. Experimentally measured forces on half projectile for various pin heights.

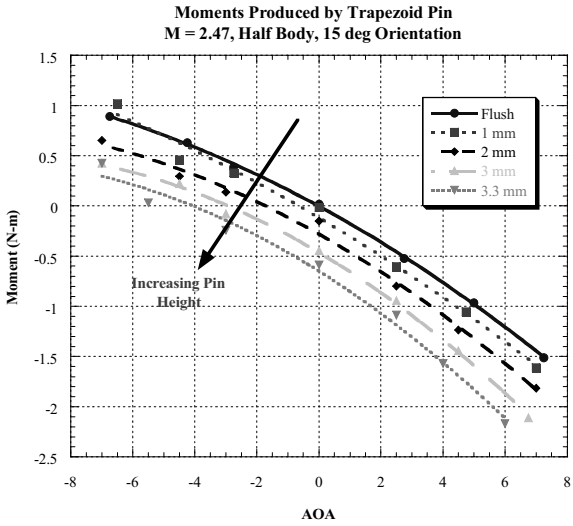


Figure 43. Experimentally measured moments on half projectile for various pin heights.

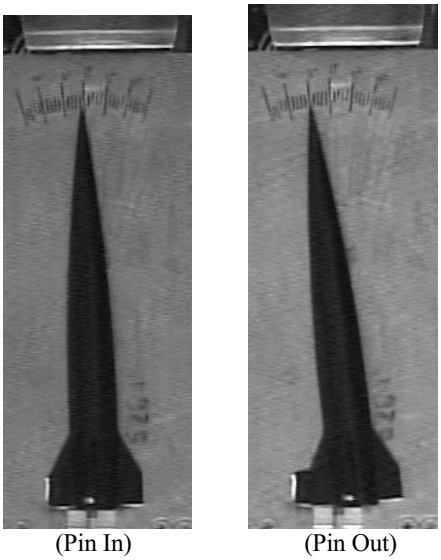


Figure 44. Free rotation of projectile with pin deployed.

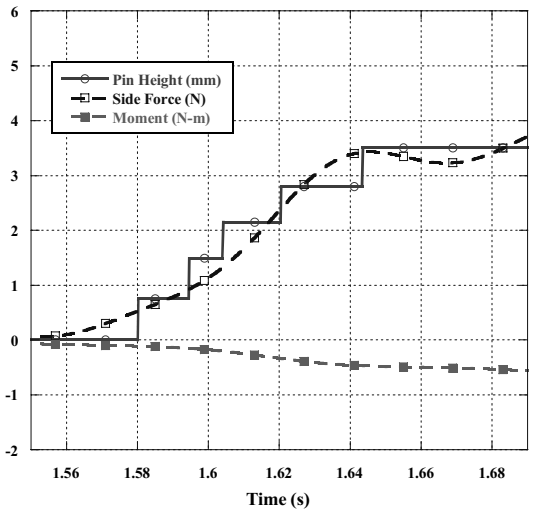


Figure 45. Time history of forces and moments for stepper motor pin insertion.

https://doi.org/10.1017/S0001924000002128 Published online by Cambridge University Press

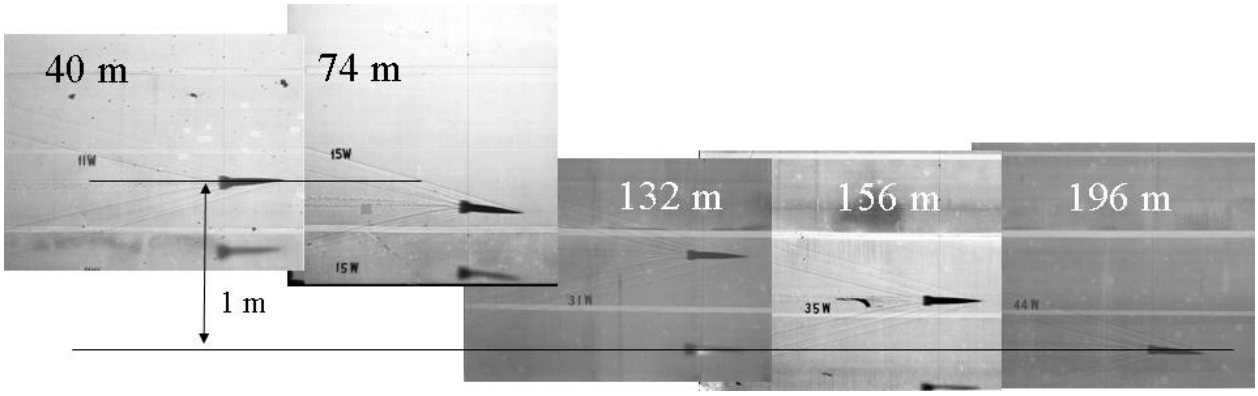


Figure 46. Divert from deployed pins in ARL spark range.

moment arm and the sensor used to measure moment as well as the pressure transducer to set the nozzle pressure ratio and the signal conditioners for the three force sensors.

The ¼ in diameter shaft that was threaded through the cg of the model passed through the ground plane and was constrained by two sets of bearings. The model, shaft and bearings were allowed to move in the cross-stream direction as they were attached to a linear air bearing. The sled of this linear slide was in turn constrained in its motion by force sensors as shown in Fig. 32, where it can also be observed that the model was constrained from rotating by another force sensor and a moment arm.

There was some concern regarding how representative of an actual projectile flying through the air that these measurements using this testing arrangement would be. In attempt to answer these valid concerns several diagnostic measurements were made. A shadowgraph system was set up to visualise the flow downstream of the jet exit. While the nozzle was designed to operate shock free at M = 2·5, it was found that the most shock free condition was actually at M = 2·475. For all the measurements made, the jet was operated at a pressure ratio to produce M = 2·475 flow with only a few weak shocks introduced by the nozzle. However, when the projectile and ground plane were placed near the jet, additional flow disturbances were introduced. Several different locations of the ground plane relative to the jet exit were tried in an effort to minimise the flow disturbances. A compromise location that introduced a weak shock off the leading edge of the ground plane yet forced the nozzle boundary-layer to go below the ground plane was used. A picture of this setup with the jet operating at condition is shown in Fig. 33. This picture, which is not a shadowgraph, shows a shock introduced by the sharp leading edge of the ground plane. While strong enough to be seen by the naked eye, this shock is nevertheless weak in the sense that the flow is only slightly affected. As seen at the bottom of Fig. 33, based on shock relations, the flow speed is reduced from M = 2·475 to M = 2·469 and the flow is turned to an angle of 0·3º. It was felt that this position of the ground plane introduced flow disturbances that could for the most part be neglected and thus all measurements were made using this setup.

9.0 ACTUATOR HARDWARE

Based on the prior experiments with pins near a fin, it was decided to use a trapezoidal pin for the scale model tests. The pin was constructed out of aluminium and designed so that it would be flush with the body of the projectile when retracted. The exposed portion of the pin was very small and its sise relative to a penny along with several dimensions is shown in Fig. 34. In this picture, one can also observe that the lower portion of the pin is much larger. This lower portion of the pin was not exposed to the flow and was used as an attachment to various pin actuation devices. To locate the pin on the projectile a hole was cut into the projectile shown in Fig. 30 near the vertical fin and into this hole one of two guide sleeves was inserted. The boattail section of the model projectile with one the guide sleeves inserted is shown in Fig. 35. Two guide sleeves were constructed so that two different orientations of the pin could be tested. The first actuator used was a manually driven micropositioner. This miniature linear slide is shown in Fig. 36 along with a scale to show its size. This positioner when combined with the pin, sleeve and mounting hardware was attached to the underside of the model. An exploded view of this assembly is shown in Fig. 37 where one can see that the actuation of the slide moves the pin in and out of the sleeve. When mounted to the model and viewed from the rear, the assembly appears as shown in Fig. 38 when the pin is retracted and as in Fig. 39 when the pin is fully deployed. The manually driven micropositioner actuator was used for the majority of the force and moment measurements as the position of the pin could be readily controlled in a repeatable and verifiable fashion.

Several electronically controlled actuator systems were also used to position the pin. The first such system used a solenoid to drive the pin up and down. It was found that this system worked well in the absence of flow, but in the presence of flow the return force was not sufficient to retract the pin. In light of this, a rack and pinion type arrangement was used in combination with a small stepper motor. This setup, shown in Fig. 40, used a stepper motor to drive a spur gear which in turn moved the rack gear up and down. The pin was attached to the rack gear and thus the position of the pin could be controlled with the stepper motor. This actuation mechanism also had the advantage of providing position feedback via an encoder on the stepper motor. While this rack and pinion arrangement provided a very useful method of controlling the pin height, tests demonstrated the pin was not deployed as rapidly as desired. For this reason, a third actuation system was developed that was electro pneumatic in nature. In this system, a solenoid was used to control the air supply to a small pneumatic cylinder. This actuation mechanism was found to have a quicker response time.

10.0 EXPERIMENTAL RESULTS

Data was acquired for the half projectile model at a Mach number of 2·47 for projectile angles of attack ranging from 7º to –7º. For each measurement, the projectile was fixed at a given angle before the flow was turned on. The force and moment data from the three force sensors was captured using a data acquisition card and customised Labview software. Both the force and moment data were found to be stationary with time as shown in Fig. 41 for a ten second period with the projectile at a 5º angle-of-attack. Since the data was found to be so stationary, the data was typically averaged over a period of one second.

https://doi.org/10.1017/S0001924000002128 Published online by Cambridge University Press

In the experimental setup used to acquire these results, the pin height was set manually using the positioner shown in Fig. 46. Data was thus rapidly acquired for multiple pin heights for a range of projectile angles of attack. It was found that the side force produced increased with increasing pin height as expected. As shown in Fig. 42, the amount of force induced by the flow interactions due to the presence of the pin ranges from 4 – 9N for the largest pin height (3·3mm). It is also seen that the force is larger as the AOA is increased (as the pin is on the windward side of the fin). The effect of the pin height on the moment is shown in Fig. 43 and these moments correspond to the forces assuming a moment arm of about 127mm. Here the differences in pin height are more pronounced, and it can be noted that a pin height of 1mm produces very little moment. This is most likely due to the fact that the pin does not extend out of the boundary layer which was optically observed to be about 1·8mm thick at this station. It is also observed that for a 3·3mm insertion, enough moment is produced such that the restoring moment of the projectile is approximately equal to the moment produced by the pin at 5º AOA. Thus the pin at 3·3mm insertion should be able to rotate the projectile to about 5º AOA.

In addition to the static pin measurements, measurements were made where the pin was inserted into the flow during the test. Two types of measurements were made; video of the projectile rotating after pin insertion and dynamic force measurements. For the videos, the moment arm was removed and the projectile was free to weathercock in the flow. The pin was initially flush and at some time later the pin was inserted to its maximum height into the flow. The projectile was found to be stable with small oscillations around zero degrees AOA at the flow conditions of M = 2·47. In Fig. 44, a snapshot from the video is shown in which the projectile was found to rotate 6º after pin insertion.

For the dynamic force measurements, the moment arm was replaced with the projectile at zero angle-of-attack. With the flow at condition (M = 2·47) the pin was deployed. Measurements of the force and moment data as well as position feedback for the pin were measured using a high speed data acquisition system. Measurements were initially made using the rack and pinion actuator where the position feedback was from the magnetic encoder off the stepper motor. The data was sampled at 250 ìs and recorded for later post processing. The data was band pass filtered, 20Hz to 4kHz, to eliminate the oscillations most likely due to turbulence in the flow. The time history of the force and moment are shown along with the encoder data in Fig. 45. It was found that the stepper motor took 78ms to fully extend the pin with much of that time occurring during the last bit of extension. While 78ms is quite fast, it is still slow compared to the flow time constants and thus it is seen that there is no noticeable lag in the measured forces with the pin deployment. With the pneumatically driven system, the pin deployment time was reduced to approximately 10ms. Similar measurements, still indicated that the flow responded more rapidly than the mechanical system, and thus it was concluded that the mechanical time to deploy the pin will drive the response time of the projectile.

11.0 GUIDANCE AND CONTROL WITH PINS OR JETS

Using the experimental results it was possible to estimate the forces that might be produced on a fin when a pin was deployed or a jet fired. Previous experimental and computational results also allowed for an estimation of the forces that might be produced on the body of a missile or projectile. Using these estimates it was possible to consider several cases of controlling the flight of a missile or projectile.

The scheme most likely to be used for roll control would involve two diametrically opposed pins or jets as shown in Error! Reference source not found.. Under the assumption that geometric similarity could be achieved in manufacturing, the forces produced would result in a pure moment about the longitudinal axis of the body. The insertion depth of the pins or strength of the jets could be altered to increase or decrease the strength of the moment produced thus providing control of the roll rate. Implementing a control of this type would also allow one to implement a bank to turn concept which might result in a simpler control scheme than a projectile that was undergoing a constant spin. Without utilising the forces developed by placing the pins near the fins, roll control is not practical using actuators of these types as the pressure forces developed on the body do not introduce a rolling moment.

For directional control, a configuration where the two pins are on the inside of adjacent fins was found to produce around 30N of force on the projectile under consideration. The moment produced and the angle to which this forces the projectile depends upon several factors. The shape of the projectile and the fin area determines the center of pressure and the moment required to maintain an angle-of-attack. Also the centre of gravity of the projectile also plays a large role as it along with the cp location determines the static margin and thus the stability of the round. Practically these variables give the designer some leeway in design.

These experiments have demonstrated the viability of using pin based actuators for guidance of supersonic fin stabilised rounds. It has been shown that the location of the pins is critical to generating the required forces though some leeway exists. The geometry of the pin also affects the force generated, and it was shown that rectangular pins generate more force than round pins.

A joint follow on effort with ARL was pursued to demonstrate the effectiveness of these guidance pins on an actual gun fired projectile. A successful demonstration of this technology was achieved in January of 2006, where several medium caliber rounds were fired at Mach numbers exceeding 4·0 in a spark range at the Aberdeen Proving Grounds. These rounds were designed to deploy two rectangular guidance pins a short time after launch. As seen in the ensemble of several spark photographs shown in Fig. 46, the round clearly diverts after the pins are deployed as it moves down the range. The dive of approximately 1m in about 150m of travel was a significant divert for this fairly stable round. After reducing the range data it was determined that a net force of about 80N was produced by the pins and that the round underwent a 14g manoeuvre. These tests validated the prior research described in this paper and served to demonstrate the utility of the guidance pins for controlling the flight of a supersonic projectile.

ACKNOWLEDGEMENTS

The authors would like to thank Sampath Palaniswamy at Metacomp who was always a joy to work with on the CFD. We also appreciate the crew at ARL for many fruitful conversations and helping out with the design of the projectile. Special thanks to Dr Sidra Silton for all her contributions on the range tests. This work was sponsored by DARPA.

REFERENCES

1. KANDEBO, S.W. New powerplant key to missile demonstrator, *Aviation Week*, 2 September 2002.
2. MARX, W.J., WESSLING III, F.C., PETERS, B.R., THIES, A., STRICKLAND, B.R. and LIANOS, D. Miniature smart munitions/guided projectiles for the objective force, 23rd Army Science Conference, December 2002.
3. WARNASH, A. and KILLEN, A. Low cost, high G, Micro Electro-Mechanical (MEMS), Inertial Measurements Unit (IMU) Program, 23rd Army Science Conference, December 2002.
4. MARGASON, R.J. Fifty years of jet in cross flow research, NASA Ames Research Center, Moffett Field, CA, USA, April 1993.
5. SPAID, F.W. and CASSEL, L.A. Aerodynamic interference induced by reaction controls, AD-775-209. Advisory Group for Aerospace Research and Development, Paris, France, December 1973.
6. HEMSCH, M.J. (ED), Tactical missile aerodynamics: General Topics, *Progress in Astronautics and Aeronautics*, 1992, **141**.

https://doi.org/10.1017/S0001924000002128 Published online by Cambridge University Press

7. HSIA, H., TAO-SZE, Equivalence of secondary injection to a blunt body in supersonic flow. United Technology Center, Sunnyvale, California, USA, *AIAA J*, October 1966, **4**, (10).
8. CHAMPIGNY, P. Lateral jet control for tactical missiles, Office National d'Etodes et de Recherches
9. SCHETZ, J. *et al*. Effects of pressure mismatch on slot injection in supersonic flow, AIAA-90-0092, Applied Physics Lab, John Hopkins University, January 1990.
10. FUJIMORI, T. *et al* Numerical prediction of two and three dimensional sonic gas transverse injections into supersonic flow, AIAA-91-0415, National Aerospace Laboratory, January 1991, Tokyo, Japan.
11. TAKAHASHI, M. and HAYASHI, A.K. Numerical study on mixing and combustion of injecting hydrogen jet in a supersonic air flow, AIAA-91-0574, Nagoya University, January 1991, Nagoya, Japan.
12. EDWARDS, J.A. Concepts behind the UK HOTLiP manoeuvring projectile program, Dstl Fort Halstead, Sevenoaks, Kent, August 2001.
13. GRAHAM, M.J. and WEINACHT, P. Numerical simulation of lateral control jets, AIAA 99-0510, 37th AIAA Aerospace Sciences Meeting, January 1999.
14. GRAHAM, M.J., WEINACHT, P. and BRANDEIS, J. A Numerical investigation of supersonic jet interaction for finned bodies, AIAA 2000-0768, 38th AIAA Aerospace Sciences Meeting, January 2000.
15. HAY, F. and MASSEY, K.C. Parametric investigation into the location and geometry of deployable pins used for guiding supersonic projectiles, AIAA 05-2-20B.
16. Metacomp Technologies, 2000: CFD++ User's Manual, Westlake Village, CA, USA.
17. GOLDBERG, U.C., PEROMIAN, O. and CHAKRAVARTHY, S. A wall-distance-free K-ε model with enhanced near-wall treatment, *J Fluids Engineering*, 1998, **120**, (3), pp 457-462.
18. SILTON, S., Comparison of predicted actuator performance for guidance of supersonic projectiles to measured range data, AIAA-2004-5195, August 2004.
19. MASSEY, K.C., GUTHRIE, K.B., and SILTON, S.I. Optimised Guidance of a Supersonic Projectile using Pin Based Actuators, 23rd Applied Aerodynamics Conference, AIAA 05-4966.

https://doi.org/10.1017/S0001924000002128 Published online by Cambridge University Press